Published in final edited form as:
Gastroenterology. 2009 September ; 137(3): 914–923. doi:10.1053/j.gastro.2009.05.050.

Saccharomyces boulardii Inhibits EGF Receptor Signaling and Intestinal Tumor Growth in *Apc*^{min} Mice

Xinhua Chen[1], **Johannes Fruehauf**[1], **Jeffrey D. Goldsmith**[2], **Hua Xu**[1], **Kianoosh K Katchar**[1], **Hon-Wai Koon**[3], **Dezheng Zhao**[1], **Efi G. Kokkotou**[1], **Charalabos Pothoulakis**[3], and **Ciarán P. Kelly**[1]

[1]Division of Gastroenterology, Department of Medicine, Beth Israel Deaconess Medical Center, Harvard Medical School, Boston, MA 02215

[2]Department of Pathology, Beth Israel Deaconess Medical Center, Harvard Medical School, Boston, MA 02215

[3]Inflammatory Bowel Disease Center, Division of Digestive Diseases, UCLA

Abstract

Saccharomyces boulardii (*Sb*) is a probiotic yeast with anti-inflammatory and antimicrobial activities and has been used for decades in the prevention and treatment of a variety of human gastrointestinal disorders. We reported previously that *Sb* modulates host inflammatory responses through down regulation of Erk1/2 MAP kinase activities both *in vitro* and *in vivo*. The aim of this study was to identify upstream mediators responsible for Erk1/2 inactivation and to examine the effects of *Sb* on tumor development in *Apc*^{Min} mice. We found that the EGF receptor was deactivated upon exposure to *Sb* leading to inactivation of both the EGFR-Erk and EGFR-Akt pathways. In human colonic cancer cells, *Sb* prevented EGF induced proliferation, reduced cell colony formation and promoted apoptosis. HER-2, HER-3 and IGF-1R were also found to be inactivated by *Sb*. Oral intake of *Sb* reduced intestinal tumor growth and dysplasia in C57BL/6J Min/+ (*Apc*^{Min}) mice. Thus, in addition to its anti-inflammatory effects, *S. boulardii* inhibits EGFR and other receptor tyrosine kinase signaling and thereby may also serve a novel therapeutic or prophylactic role in intestinal neoplasia.

Introduction

Saccharomyces boulardii (*Sb*) is a non-pathogenic yeast that has been used for many years as a probiotic agent to prevent or treat a wide variety of human gastrointestinal disorders of diverse etiologies[1-3]. Preclinical and experimental studies of *S. boulardii* have demonstrated anti-inflammatory, antimicrobial, enzymatic, metabolic and anti-toxin activity[4-7]. *S. boulardii* appears to exert its therapeutic effect by multiple mechanisms and to influence several important facets of intestinal host-pathogen interaction. We and others have reported that *Saccharomyces boulardii* acts through modulation of host signaling pathways that regulate the intestinal mucosal inflammatory response. Particularly, the Erk1/2 MAP kinase pathway is down-regulated by *Sb* both *in vitro* and *in vivo*[8, 9].

Corresponding Author: Ciarán P. Kelly, e-mail: ckelly2@bidmc.harvard.edu.

MAP kinase pathways are located downstream of many growth-factor receptors, including the Epidermal Growth Factor Receptor (EGFR), through the Raf /MEK /ERK cascade [10]. Therefore, we hypothesized that *Sb* inhibited Erk activation via an upstream effect on EGFR or other receptor tyrosine kinase signaling. Our data in this study suggested that EGFR signaling is inactivated by *Sb*. It has been well characterized that activation of EGFR results in enhanced cell proliferation, invasion and tumor metastasis, as well as inhibition of apoptosis [11]. Signaling pathways that emerge from EGFR activation are critical in colon cancer biology [12]13. EGFR inhibitors have demonstrated clinical benefit for colorectal cancer treatment [14, 15]. Since *Sb* has shown beneficial effects in a series of gastrointestinal disorders, we wanted to know if *Sb* has potential anti-cancer properties by examining whether the effects of *Sb* on EGFR signaling can influence proliferation and apoptosis of colon cancer cells *in vitro*, as well as intestinal tumor growth in Apc^{Min} mice *in vivo*.

Results

SbS inactivates EGFR-Mek-Erk pathway signaling in colonic cancer cells

We have reported that Erk1/2 MAP kinase activation is inhibited by SbS *in vitro* and *in vivo* 9. We hypothesized that EGFR signaling might be affected upstream to Erk. After varying periods of time (0 to 180 minutes) of exposure to SbS, HT29 cells were harvested, cell extracts prepared and Western blotting performed using either phospho- specific or total EGFR, MEK1/2, ERK1/2 antibodies. We found that SbS markedly reduced EGFR phosphorylation (Tyr1173) with a rapid onset of effect (1 minute). Reversibility of the SbS inhibitory effect was apparent with some return of EGFR phosphorylation becoming evident at later time points (Figure 1a). Phospho-Mek1/2, a downstream signaling molecule to EGFR but an upstream kinase to Erk1/2, also lost much of its activity after 5 minutes of SbS exposure. As expected p-Erk1/2 activity was also significantly decreased following de-phosphorylation of EGFR and MEK1/2 (Figure 1a). These findings are consistent with the theory that phospho-Erk1/2 is reduced by SbS through effects on the EGFR-Mek-Erk pathway. This provided a mechanism to account for the effects of SbS on Erk1/2 MAP kinase activity as described in our previous studies [9]. As other receptor tyrosine kinases such as insulin-like growth factor-1 receptor (IGF-1R) and ErbB family members including HER-2 and HER-3 also stimulate MAP kinase signaling, we examined HER-2, HER-3 and IGF-1R activation level in SbS treated HCT-116 or HT29 cells. We found p-HER-2, p-HER-3 and p-IGF-1R, are all inactivated by SbS in similar fashion as p-EGFR (Figure 1b). Other signaling kinases, such as phospho-CamKII (Figure 1a) and PKC family members including phsphorylated forms of PKC-alpha, PKC-delta, PKC-theta and PKCmu were not affected by SbS (data not shown), indicating an effect on receptor tyrosine kinases including EGFR, HER-2, Her-3 and IGF-1R rather than global dephosphorylation and inactivation.

To examine if SbS inhibits ligand-induced activation of these receptor tyrosine kinases, SW480 or HCT-116 cells were treated with 10ng/ml recombinant EGF ligand or 100 ng/ml recombinant Neuregulin (NRG1) ligand, with or without the presence of SbS at various time points. As shown in Figure 1c, SbS completely blocked EGF-induced EGFR activation and attenuated NRG1-induced HER-2 and HER-3 activation.

SbS inhibits colon cancer cell proliferation and cell colony formation

The effect of SbS on EGFR signaling led us to examine whether cancer cell proliferation may be altered as a consequence of EGFR deactivation. Using the MTS assay, semi-confluent colonic adenocarcinoma HT29 cells were stimulated with 10ng/ml EGF in the presence or absence of SbS for 24 hours. We found that SbS abolished EGF-stimulated relative cell number increase ($p<0.001$) (Figure 2a). Furthermore, BrdU labeling was used in colorimetric immunoassay for the quantification of cell proliferation. As shown in Figure 2b, SbS

significantly reduced EGF induced cell proliferation ($p<0.01$) quantified by incorporation of BrdU.

We next determined the effect of SbS in cell survival using the colony formation assay. HT29 cells were grown in DMEM containing 10% serum in the absence or presence of different concentrations of SbS for 10-20 days. SbS showed a dose dependent inhibition of HT29 cell colony formation. At dilutions as low as 1/64, this inhibitory effect was still evident and statistically significant (Figure 2b). Thus, SbS reduces proliferation and colony formation of HT29 cells *in vitro*. This inhibition was almost identically repeated in SW480 cells treated by the same dilutions of SbS (data not shown).

SbS inactivates phopho-Akt and induces cancer cell apoptosis

Since Akt is a key signaling molecule for cell survival and is also a downstream molecule to the EGFR, we next tested whether Akt was also affected by SbS. After varying periods (0 - 240 min) of exposure to SbS, cells were lysed and samples tested by Western blotting for Akt phosphorylation. After 15 minutes of exposure to SbS and thereafter Akt phosphorylation was markedly decreased whereas total Akt remain unchanged (Figure 3a).

In view of these effects on Akt activations we next determined whether SbS affects cell apoptosis. We evaluated apoptosis by flow cytometry, caspase assay and tunnel staining. For flow cytometry, HT29 cells were treated with or without SbS for different time periods (4, 8, 12 hours), and then stained by propidium iodide followed by flow cytometric analysis. We found that SbS treatment increased the sub-G1 cell fraction in a time-dependent manner (control 12%, SbS treated 4 hr 22%, 8 hr 28%, 12 hr 40%), suggesting that SbS promoted HT29 cancer cell death (Figure 3b).

HT29 cells treated with SbS for 4 hours at varying dilutions (1/2 to 1/64) were then tested using a homogenous caspase assay kit (Roche Diagnostics). We found that SbS induced caspase activity in a dose-dependent fashion. Even at the 1/64 dilution, the induction of caspase activity was significantly higher compared to negative control cells (Figure 3c). Furthermore, we demonstrated that SbS induces apoptosis by tunnel staining as shown in Figure 3d. The average percentage of positively stained cells in those treated with SbS (1/8 dilution) is 32.0±8.5%, vs. control cells 1.5±0.5%, ($p<0.01$). These data indicate that SbS inactivates phospho-Akt and induces cancer cell apoptosis.

To confirm the role of SbS-regulated EGFR and Akt in apoptosis, we transiently transfected HT29 cells with constitutively active myr-Akt using the empty pUSE vector as control. Treatment of transected cells by SbS at 1/2 dilution for 30 minutes decreased endogenous p-Akt signal whereas ectopic myr-Akt remained intact. Adding EGF (20ng/ml) to SbS treated cells reversed the p-Akt signal reduction induced by SbS (Figure 3e). HT 29 cells transiently transfected with vector or myr-Akt were treated with different dilutions of SbS for 12 hours and the apoptotic rate of cells was analyzed by Tunel staining,. As shown in Figure 3f, ectopic myr-Akt expression inhibited Sb-mediated apoptosis at all SbS dilutions. ($P<0.01$). Stimulation by 20ng/ml EGF ligand also significantly reduced SbS-induced apoptosis at 1/4 dilution of SbS. ($P<0.01$). (Figure 3f)

Oral intake of *Sb* inhibited tumor growth in Apc^{Min} mice

To test whether Sb inhibits cancer growth *in vivo*, we administrated *Sb* to C57BL6/min/+ (Apc^{Min}) mice daily from age 7 weeks until 16 weeks of age. Mice were then sacrificed and the 10 cm section of the distal small intestine was harvested, from which we measured the number, size and grade of dysplasia in intestinal tumors. We found that orally administered *Sb* led to a significant reduction in the number (mean ± SE: 29.7 ± 4.8 for control (n=6) versus

16.4 ± 3.0 for *Sb* treated (n=8), p=0.03), diameter (3.3 ± 0.2 mm versus 2.7 ± 0.2 mm, p=0.03) and total surface area (102 ± 21.7 mm^2 versus 44.5 ± 9.4 mm^2, p=0.02) of intestinal tumors in the Apc^{Min} mice (Figure 4a).

The tumors in the Apc^{Min} mice were categorized as showing low or high grade dysplasia, using a system based on human colonic carcinoma profiles. *Sb*-treated mice had a significantly lower score for low-grade dysplasia compared to control mice (p=0.01). Scores for high grade dysplasia were also lower than in the control group but this difference did not reach statistical significance (p=0.12, Figure 4b). Representative images from H&E stained small intestines demonstrated reduced numbers of polyps (Figure 4c).

Immunochemistry using antibodies against PCNA, a cell proliferation marker, showed that *Sb*-treated Apc^{Min} mice had fewer proliferative cells in their tumors (PCNA positive staining) compared to control mice. Figure 5 shows representative images from both *Sb* treated Apc^{Min} mice and control mice. PCNA positive cells within the tumor are 66% in control mice, compared to 37% in *Sb*-treated mice (66 ± 14% vs. 37 ± 20 %, p<0.01), indicating that cell proliferation is attenuated in tumors of *Sb*-treated mice (Figure 5a). The average percentage of phospho-EGFR (Tyr1173) positive cells per high power field in *Sb*-treated mice vs. control mice are 6.5 ± 2.8 % vs. 17 ± 5.5 %, p<0.05. The average percentage of p-Akt strongly stained cells per high power field from *Sb*-treated mice vs. control mice are 49.6 ± 5.4% vs. 70.4 ± 4.5%, p=0.01. Representative images of p-EGFR and p-Akt in Figure 5b&c showed that both activation molecules are less evident in treated mice, indicating that the effects of *Sb* on phospho-EGFR and phospho-Akt is also evident *in vivo*, consistent with the results of our *in vitro* experiments with HT-29 cells (Figure 1 and 3a). Tunel staining of intestinal tissues and control Apc^{min} mice demonstrated a significant increase of apoptotic cells from *Sb*-treated mice. The average percentages of apoptotic cells per high power field are 15 ± 3.0 % in *Sb*-treated mice, vs. 4.5 ± 2.3 % in control mice respectively. p<0.01. Representative images are shown in Figure 5d.

Discussion

One of the beneficial effects of *Saccharomyces boulardii* is its ability to reduce intestinal inflammatory responses. Erk1/2 MAP kinases, a major modulator of host inflammatory responses, are negatively regulated by *Sb* [5, 9]. Here we report that *Sb* inhibits Erk kinase activity through effects on the EGFR/Mek pathway. The active (phosphorylated) form of EGFR rapidly loses its activity upon exposure to SbS, which leads to the downstream inactivation of p-Mek and p-Erk as well as p-Akt. Dephosphorylation of p-EGFR is not due to a toxic effect of SbS since, as we previously reported, the inhibitory effect of SbS is fully reversible[16]. The fact that p-EGFR, p-Mek1/2 and p-Erk1/2 slowly recover their activities, as indicated by our Western blot data, is entirely consistent with this finding.

SbS prevented cancer cell colony formation, reduced EGF-mediated cell proliferation and increased apoptosis. The *in vitro* effects are consistent with inhibition of the EGFR and Akt pathways. The inhibitory effect of *Sb* on p-EGFR and p-Akt appears to occur *in vivo* also. Immunostaining intensity of both p-EGFR and p-Akt decreased in *Sb* treated Apc^{Min} mice. Furthermore, Apc^{Min} mice treated with *Sb* demonstrated beneficial effects compared to non-treated mice by showing a 50% decrease in tumor number and a substantial drop in tumor volume. This suggests that *S. boulardii* may have a beneficial role in preventing or treating intestinal adenomatous polyps and/or adenocarcinoma.

Aberrant activation of EGFR has been shown to be critical for the maintenance of malignancy in a number of solid tumors, including colorectal cancer [17, 18]. Interference with the activation of EGFR and other growth factor receptors represents a promising strategy for novel and

selective anticancer therapies [19]. In the *Apc*^{Min} mouse model, it has been shown that EGFR activity is important in the establishment of intestinal tumors and *Apc* deficiency is associated with increased EGFR activity [20, 21]. Our *in vitro* cell signaling studies indicated SbS inactivates other receptor tyrosine kinases including HER-2, HER-3 and IGF-1R besides EGFR, which are all involved in cell proliferation and apoptosis, and commonly overexpressed in many cancers and play important roles in neoplasia [22-24]. In our hands, immunohistochemical staining of phospho-IGF-1R yielded no staining pattern in tumors of *Apc*^{min} mice. However, phospho-EGFR showed clear differences between *Sb*-treated and control mice. Our data also suggested both EGF ligand stimulation and constitutively active Akt expression inhibit the pro-apoptotic effect of SbS, indicating the direct involvement of EGFR-Akt pathway in *Sb*-mediated apoptosis. The roles of IGF-1R and HER-2 & 3 in *Sb*-mediated cell proliferation and apoptosis, as well as tumor reduction in *Apc*^{min} mice need to be further addressed in our future studies. However, the inhibitory effect of *Sb* on EGFR activity, with downstream effects on Akt, at least in part explains its beneficial effect in reducing tumor growth.

As yet, the detailed mechanism of how SbS inactivates both basal and ligand induced activation of EGFR and HER-2 & 3 is unknown. Compartmentalization of receptor tyrosine kinases including EGFR into sub-domains of the cell membrane is an important control mechanism for signaling [25-27]. One hypothesis is that SbS may alter the membrane localization of receptor tyrosine kinases and their association with lipid rafts. This may explain the effects of *Sb* on a variety of receptor tyrosine kinases. Nonetheless, our findings indicate that the yeast *S. boulardii* can exert anti-cancer effects through inactivation of growth receptors. Receptor tyrosine kinases are key molecular targets for cancer therapy and, to our knowledge, this is the first report of major receptor tyrosine kinase inactivation by a probiotic microorganism. Several animal studies showed a reduction in chemically induced colorectal tumor incidence accompanying probiotic bacteria administration, however the mechanisms were not well understood [28-30]. Our findings that *Sb* inhibits EGFR signaling and reduces tumor growth in *Apc*^{Min} mice provide a novel mechanism for probiotic actions against cancer. *S. boulardii* appears to exert its beneficial effects by multiple potential mechanisms of action [31], including neutralization of bacterial virulence factors [4, 32], interference with bacterial adhesion [33], strengthening of enterocyte tight junctions [34], enhancement of the mucosal immune response [35, 36], altering immune cell redistribution [37] and modulating inflammatory signaling pathways of the host [8, 9]. Given the complicated picture of probiotic actions, we cannot exclude other potential mechanisms that may explain the anti-cancer phenomenon of *Sb*. Besides receptor tyrosine kinase inactivation, the anti-inflammatory properties of *Sb* or possible gut flora changes due to *Sb* administration in *Apc*^{min} mice may also impact intestinal tumor development. Further studies are needed to explore these potential mechanisms. Nevertheless, with decades of usage profile in treating gastrointestinal disorders, the clinical effects of *Saccharomyces boulardii* on prevention and treatment of colon polyps and colon cancer clearly warrant further investigation.

Materials and Method

Cells and Reagent

HT29, SW480 and HCT-116 cells were obtained from ATCC. HT29 and SW 480 cells were cultured in DMEM, whereas HCT-116 in McCoy's 5A modified media, supplemented with 10% (vol/vol) FBS, 2 mM L-glutamine (GIBCO), 100 U/ml penicillin, and 100 μg/ml streptomycin in a 5% CO_2 incubator at 37°C. Recombinant human (rh) Epidermal Growth Factor (EGF), recombinant human Neuregulin (NRG-1) were purchased from R & D Systems (Minneapolis, MN). Antibodies against Erk, MEK, CamKII kinases, PKCs, EGFR, IGF-1R, HER-2, HER-3 and Akt, phosphorylated and/or non-phosphorylated forms, were purchased from Cell Signaling Technology (Beverly, MA). DNA constructs myr-Akt-pUSE and pUSE

empty vector were gifts from Dr. Grant D Stewart from University of Edinburgh. Preparation of *Saccharomyces boulardii* culture supernatant (SbS) was done as previously described [9]. Briefly, lyophilized *Sb* (Biocodex Laboratories, France) was cultured in RPMI 1640 cell culture medium (100mg/ml) for 24 hours in 37°C. The suspension was then centrifuged at 9000g for 15 minutes and the supernatant collected. The supernatant was then passed through a 0.22 mm filter (Fisher Scientific) and then a 10 kDa cutoff filter (Millipore, MA).

Western blot analysis

HT29, SW480 or HCT-116 cells were incubated with *SbS* at 1:1 dilution for different time periods at different conditions. Treated cells were then lysed in a lysis buffer (62.5 mM Tris-HCl, 10% glycerol, 2% SDS, 0.01% bromphenol blue, and 1% 2-mercaptoethanol). Equal amounts of cell extract were fractionated by 10% SDS-PAGE, and proteins were transferred onto nitrocellulose membranes (Bio-Rad) at 300 mA for 3 h. Membranes were blocked in 5% nonfat dried milk in TBST (50 mM Tris, pH 7.5, 0.15 M NaCl, 0.05% Tween 20) and then incubated with antibodies directed against phopho- or nonphosphorylated forms of ERK1/2, MEK1/2, HER-2, HER-3, IGF-1R (Cell Signaling, MA) and EGFR (Santa Cruz Technology). Membranes were washed with TBST and incubated with horseradish peroxidase-labeled secondary antibodies for 1 h. The peroxidase signal was detected by Supersignal chemiluminescent substrate (Pierce), and the image of the signal was recorded by exposure to x-ray film (Fujifilm, Tokyo, Japan).

Colony formation assay and cell proliferation assays

HT29 and SW480 cells were seeded at 1,000 cells per well in six-well plates and allowed to attach for 48 h. SbS was diluted in DMEM at different concentrations and added directly to cell culture wells. Cultures were observed daily for 10–20 days and then were fixed and stained with modified Wright-Giemsa stain (Sigma). Colonies of 30 cells were scored as survivors [38]. Cells were maintained at 37°C in 5% CO_2 in complete humidity. HT29 cells were cultured in DMEM supplemented with 10% (vol/vol) FBS and 2 mM L-glutamine (GIBCO). Cell proliferation assays were carried out using both MTS assay kit (Promega) and BrdU colorimetric kit (Roche Applied Science) following manufacture's instructions.

Cell transfection

90-100% confluent HT29 cells grown in 12-well dishes or 4 Chamber Polystyrene Vessel Glass Slides were transfected with pUSE empty vector or pUSE-myr-Akt plasmids using Lipofecatmine 2000 (Invitrogen, Inc.). 24 hour after transfection, cells were treated with SbS for 30 mins before being lysed for Western blot analysis, or treated over night for TUNEL staining.

Apoptosis assays

Tunel assay was carried out in both HT29 cell culture and intestinal tissues using TUNEL Apoptosis Detection Kit (Upstate Biotechnology Inc., Lake Placid, NY) according to the manufacturer's instructions. For flow cytometry, adherent HT29 cells were released by treatment with 0.25% trypsin. Each sample was fixed overnight with 70% ethanol at 4°C. Cells were rehydrated with phosphate-buffered saline (PBS) and then stained with 10% propidium iodide (PI) in 100 U/mL of ribonuclease in PBS for 60 minutes at room temperature. Cells were filtered through 35-μm filters before analysis. The flow cytometer was configured to track the number of events with the FL2 parameter (FACScan; Becton Dickinson, Lincoln Park, NJ). The DNA content was analyzed using a nonlinear least-squares algorithm. Caspase activation was measured with a fluorimetric homogeneous caspase assay kit (Roche Applied Science).

Apc^{Min} mice

C57BL/6J Min/+ (*Apc*^{Min}) mice were obtained from the Jackson Laboratory (Bar Harbor, ME) at age 7 weeks. *Sb* was administrated daily in their drinking water 3×10^8 CFU per ml and 3 times each week by oral gavage at a dose of 6×10^8 CFU for 9 weeks. Mice were sacrificed at 16 weeks of age. Intestinal tumor number was counted in the distal 10 cm of the small intestine using Methylene Blue in PBS (0.05%). Tumor sizes were measured by external caliper and taken as diameter to calculate total areas. Proximal sections of the rest of the small intestine (remaining section after usage of 10cm distal part) were fixed and used for immunohistochemistry. Grade of dysplasia was measured by a blinded pathologist using a simple grading system based on the criteria for adenomatous change in the human colon: high-grade vs. low-grade dysplasia, where low-grade dysplasia showed nuclear elongation with a sessile or villous architecture, and high-grade dysplasia showed a cribriform growth pattern with loss of nuclear polarity and nuclear rounding. Relevant tissues were fixed overnight in 10% neutral-buffered formalin for immunohistochemistry. Animal studies were approved by the Institutional Animal Care and Use Committee.

Immunohistochemistry and imaging analysis

Immunohistochemical staining was done on fixed intestinal tissues in Beth Israel Deaconess Medical Center Immunohistochemistry Core Facility using specific antibodies against PCNA, phospho-EGFR, and phosphor-Akt and counterstained with hematoxylin. Images were viewed under light microscopy (Eclipse E800, Nikon) by using a plain Apo 40×/0.95 objective, imported via a SPOT Insight camera (Diagnostic Instruments, Sterling Heights, MI), and stored digitally using SPOT software (Diagnostic Instruments). For semi-quantitative analysis of immunohistochemistry imaging, microscopic views of 10 random tumors from each animal group were randomly chosen and examined by a blinded observer. On each microscopic field, cells positively stained by p-EGFR or p-Akt were counted, as well as the total number of cells by haemotoxylin staining. In the case of quantifying Tunel stained colon tumor images, cells positively stained by FITC and total cells by DAPI were counted. The percentage of positively staining cells on each high power field was calculated for both groups and statistically analyzed.

Statistical Analyses

Results were expressed as mean ± S.E. Data were analyzed using the SIGMA-STAT™ professional statistics software program (Jandel Scientific Software, San Rafael, CA). Analyses of variance with protected *t* test were used for intergroup comparison.

Acknowledgments

This work was supported by NIH grants PO1 DK 33506 (to CPK), and Crohn's & Colitis Foundation of America (research fellowship to XC).

References

1. Elmer GW, Surawicz CM, McFarland LV. Biotherapeutic agents. A neglected modality for the treatment and prevention of selected intestinal and vaginal infections. Jama 1996;275:870–6. [PubMed: 8596226]
2. Sullivan A, Nord CE. The place of probiotics in human intestinal infections. Int J Antimicrob Agents 2002;20:313–9. [PubMed: 12431865]
3. Guslandi M, Mezzi G, Sorghi M, Testoni PA. Saccharomyces boulardii in maintenance treatment of Crohn's disease. Dig Dis Sci 2000;45:1462–4. [PubMed: 10961730]
4. Castagliuolo I, LaMont JT, Nikulasson ST, Pothoulakis C. Saccharomyces boulardii protease inhibits Clostridium difficile toxin A effects in the rat ileum. Infect Immun 1996;64:5225–32. [PubMed: 8945570]

5. Czerucka D, Dahan S, Mograbi B, Rossi B, Rampal P. Saccharomyces boulardii preserves the barrier function and modulates the signal transduction pathway induced in enteropathogenic Escherichia coli-infected T84 cells. Infect Immun 2000;68:5998–6004. [PubMed: 10992512]
6. Czerucka D, Roux I, Rampal P. Saccharomyces boulardii inhibits secretagogue-mediated adenosine 3′,5′-cyclic monophosphate induction in intestinal cells. Gastroenterology 1994;106:65–72. [PubMed: 8276210]
7. Dalmasso G, Cottrez F, Imbert V, Lagadec P, Peyron JF, Rampal P, Czerucka D, Groux H. Saccharomyces boulardii Inhibits Inflammatory Bowel Disease by Trapping T Cells in Mesenteric Lymph Nodes. Gastroenterology 2006;131:1812–1825. [PubMed: 17087945]
8. Dahan S, Dalmasso G, Imbert V, Peyron JF, Rampal P, Czerucka D. Saccharomyces boulardii interferes with enterohemorrhagic Escherichia coli-induced signaling pathways in T84 cells. Infect Immun 2003;71:766–73. [PubMed: 12540556]
9. Chen X, Kokkotou EG, Mustafa N, Bhaskar KR, Sougioultzis S, O'Brien M, Pothoulakis C, Kelly CP. Saccharomyces boulardii inhibits ERK1/2 mitogen-activated protein kinase activation both in vitro and in vivo and protects against Clostridium difficile toxin A-induced enteritis. J Biol Chem 2006;281:24449–54. [PubMed: 16816386]
10. Fang JY, Richardson BC. The MAPK signalling pathways and colorectal cancer. The Lancet Oncology 2005;6:322–327. [PubMed: 15863380]
11. Jimeno A, Hidalgo M. Pharmacogenomics of epidermal growth factor receptor (EGFR) tyrosine kinase inhibitors. Biochim Biophys Acta 2006;1766:217–29. [PubMed: 17045403]
12. de Castro-Carpeno J, Belda-Iniesta C, Casado Saenz E, Hernandez Agudo E, Feliu Batlle J, Gonzalez Baron M. EGFR and colon cancer: a clinical view. Clin Transl Oncol 2008;10:6–13. [PubMed: 18208787]
13. Calonghi N, Pagnotta E, Parolin C, Mangano C, Bolognesi ML, Melchiorre C, Masotti L. A new EGFR inhibitor induces apoptosis in colon cancer cells. Biochem Biophys Res Commun 2007;354:409–13. [PubMed: 17227671]
14. Ponz-Sarvise M, Rodriguez J, Viudez A, Chopitea A, Calvo A, Garcia-Foncillas J, Gil-Bazo I. Epidermal growth factor receptor inhibitors in colorectal cancer treatment: what's new? World J Gastroenterol 2007;13:5877–87. [PubMed: 17990353]
15. Marshall J. Clinical implications of the mechanism of epidermal growth factor receptor inhibitors. Cancer 2006;107:1207–18. [PubMed: 16909423]
16. Sougioultzis S, Simeonidis S, Bhaskar KR, Chen X, Anton PM, Keates S, Pothoulakis C, Kelly CP. Saccharomyces boulardii produces a soluble anti-inflammatory factor that inhibits NF-kappaB-mediated IL-8 gene expression. Biochem Biophys Res Commun 2006;343:69–76. [PubMed: 16529714]
17. Jiang D, Yang H, Willson JK, Liang J, Humphrey LE, Zborowska E, Wang D, Foster J, Fan R, Brattain MG. Autocrine transforming growth factor alpha provides a growth advantage to malignant cells by facilitating re-entry into the cell cycle from suboptimal growth states. J Biol Chem 1998;273:31471–9. [PubMed: 9813060]
18. Huang SM, Harari PM. Epidermal growth factor receptor inhibition in cancer therapy: biology, rationale and preliminary clinical results. Invest New Drugs 1999;17:259–69. [PubMed: 10665478]
19. Nautiyal J, Rishi AK, Majumdar AP. Emerging therapies in gastrointestinal cancers. World J Gastroenterol 2006;12:7440–50. [PubMed: 17167831]
20. Roberts RB, Min L, Washington MK, Olsen SJ, Settle SH, Coffey RJ, Threadgill DW. Importance of epidermal growth factor receptor signaling in establishment of adenomas and maintenance of carcinomas during intestinal tumorigenesis. Proc Natl Acad Sci U S A 2002;99:1521–6. [PubMed: 11818567]
21. Moran AE, Hunt DH, Javid SH, Redston M, Carothers AM, Bertagnolli MM. Apc deficiency is associated with increased Egfr activity in the intestinal enterocytes and adenomas of C57BL/6J-Min/+ mice. J Biol Chem 2004;279:43261–72. [PubMed: 15294912]
22. Stern DF. ERBB3/HER3 and ERBB2/HER2 duet in mammary development and breast cancer. J Mammary Gland Biol Neoplasia 2008;13:215–23. [PubMed: 18454306]
23. Pollak M. Insulin and insulin-like growth factor signalling in neoplasia. Nat Rev Cancer 2008;8:915–28. [PubMed: 19029956]

24. LeRoith D, Roberts CT Jr. The insulin-like growth factor system and cancer. Cancer Lett 2003;195:127–37. [PubMed: 12767520]
25. Le Roy C, Wrana JL. Clathrin- and non-clathrin-mediated endocytic regulation of cell signalling. Nat Rev Mol Cell Biol 2005;6:112–26. [PubMed: 15687999]
26. Miljan EA, Bremer EG. Regulation of growth factor receptors by gangliosides. Sci STKE 2002;2002:RE15. [PubMed: 12454318]
27. Thiel KW, Carpenter G. ErbB-4 and TNF-alpha converting enzyme localization to membrane microdomains. Biochem Biophys Res Commun 2006;350:629–33. [PubMed: 17027649]
28. Hirayama K, Rafter J. The role of probiotic bacteria in cancer prevention. Microbes Infect 2000;2:681–6. [PubMed: 10884619]
29. Rafter J. Probiotics and colon cancer. Best Practice & Research Clinical Gastroenterology 2003;17:849–859. [PubMed: 14507593]
30. Brady LJ, Gallaher DD, Busta FF. The Role of Probiotic Cultures in the Prevention of Colon Cancer. J Nutr 2000;130:410S–414S. [PubMed: 10721916]
31. Chen, X.; Kelly, C. Saccharomyces spp. In: Versalovic, J.; Wilson, M., editors. Therapeutic Micriobiology: Probiotics and Related Strategies. Vol. 1st. Washington, DC: ASM Press; 2008. p. 51-60.
32. Pothoulakis C, Kelly CP, Joshi MA, Gao N, O'Keane CJ, Castagliuolo I, Lamont JT. Saccharomyces boulardii inhibits Clostridium difficile toxin A binding and enterotoxicity in rat ileum. Gastroenterology 1993;104:1108–15. [PubMed: 8462799]
33. Gedek BR. Adherence of Escherichia coli serogroup O 157 and the Salmonella typhimurium mutant DT 104 to the surface of Saccharomyces boulardii. Mycoses 1999;42:261–4. [PubMed: 10424093]
34. Philpott DJ, McKay DM, Sherman PM, Perdue MH. Infection of T84 cells with enteropathogenic Escherichia coli alters barrier and transport functions. Am J Physiol 1996;270:G634–45. [PubMed: 8928793]
35. Buts JP, Bernasconi P, Vaerman JP, Dive C. Stimulation of secretory IgA and secretory component of immunoglobulins in small intestine of rats treated with Saccharomyces boulardii. Digestive Diseases And Sciences 1990;35:251–256. [PubMed: 2302983]
36. Qamar A, Aboudola S, Warny M, Michetti P, Pothoulakis C, LaMont JT, Kelly CP. Saccharomyces boulardii stimulates intestinal immunoglobulin A immune response to Clostridium difficile toxin A in mice. Infection And Immunity 2001;69:2762–2765. [PubMed: 11254650]
37. Dalmasso G, Cottrez F, Imbert V, Lagadec P, Peyron JF, Rampal P, Czerucka D, Groux H, Foussat A, Brun V. Saccharomyces boulardii inhibits inflammatory bowel disease by trapping T cells in mesenteric lymph nodes. Gastroenterology 2006;131:1812–25. [PubMed: 17087945]
38. Li Y, Sun X, LaMont JT, Pardee AB, Li CJ. Selective killing of cancer cells by beta -lapachone: Direct checkpoint activation as a strategy against cancer. PNAS 2003;100:2674–2678. [PubMed: 12598645]

a)

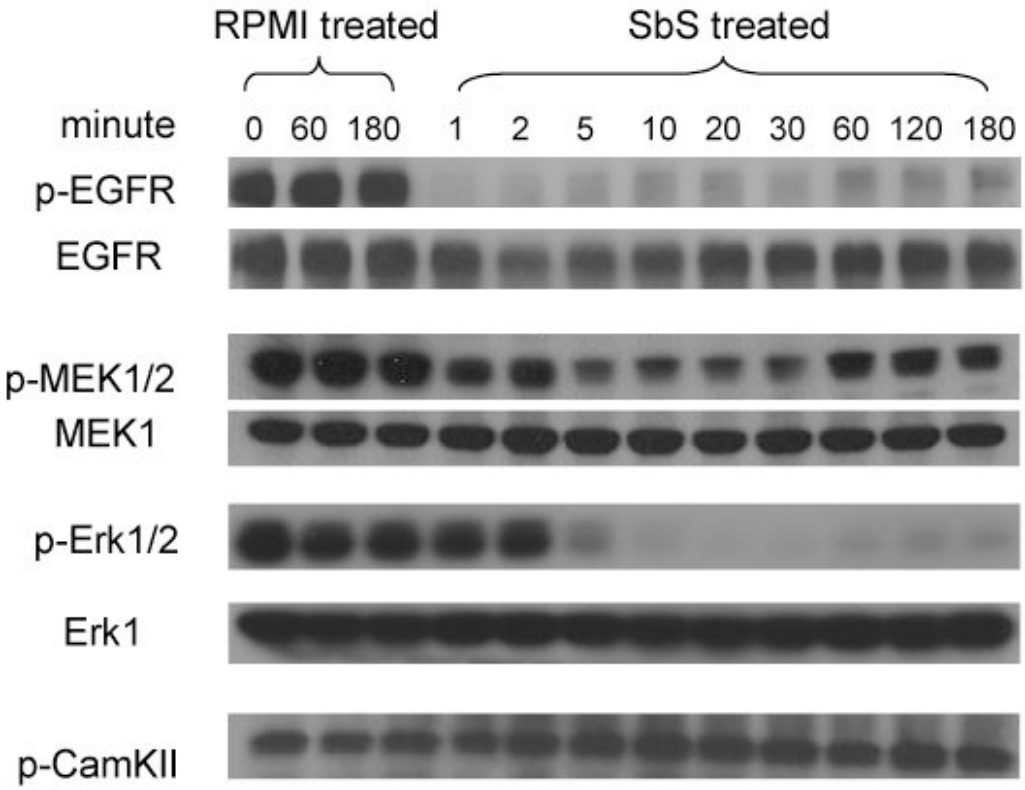

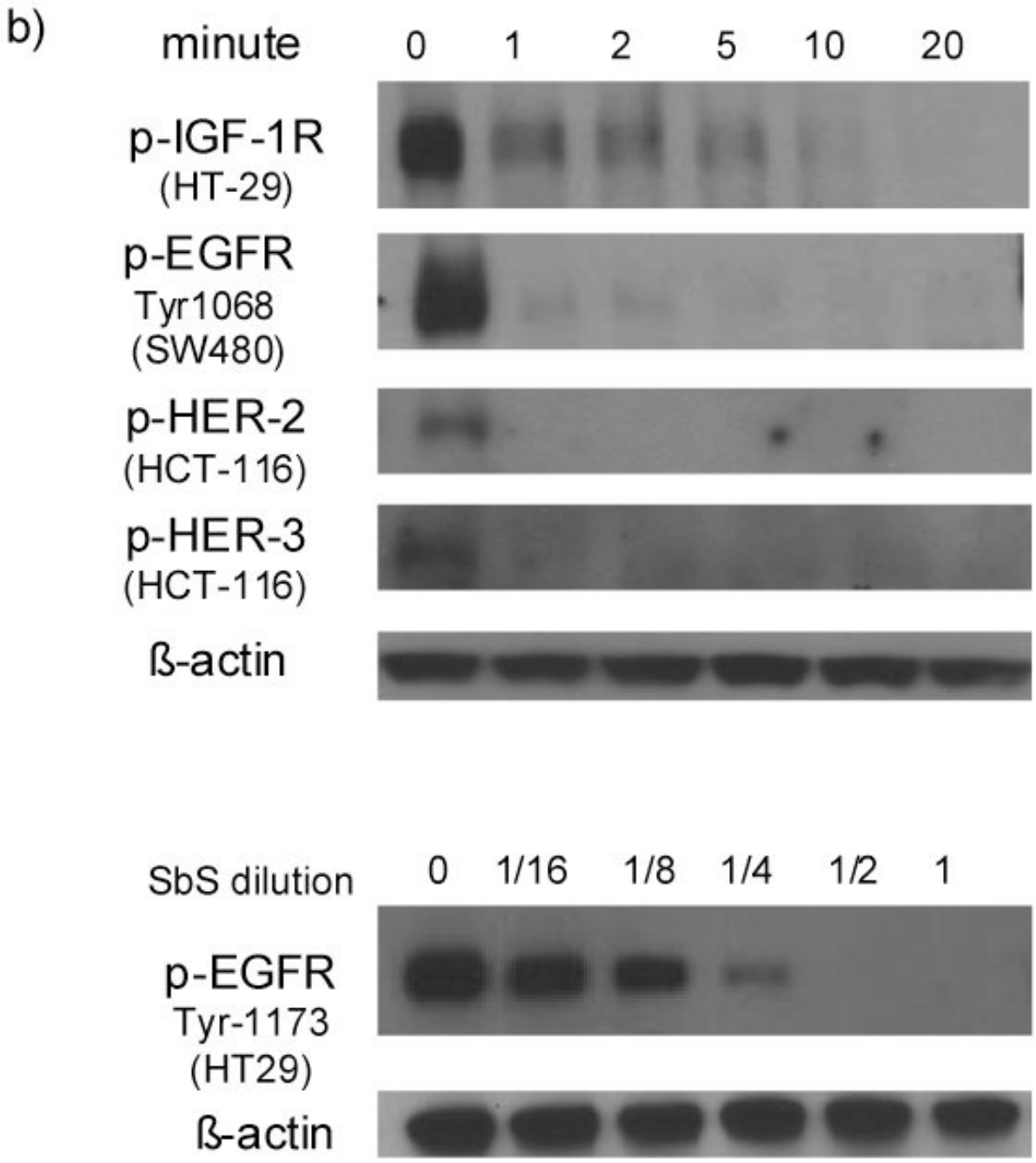

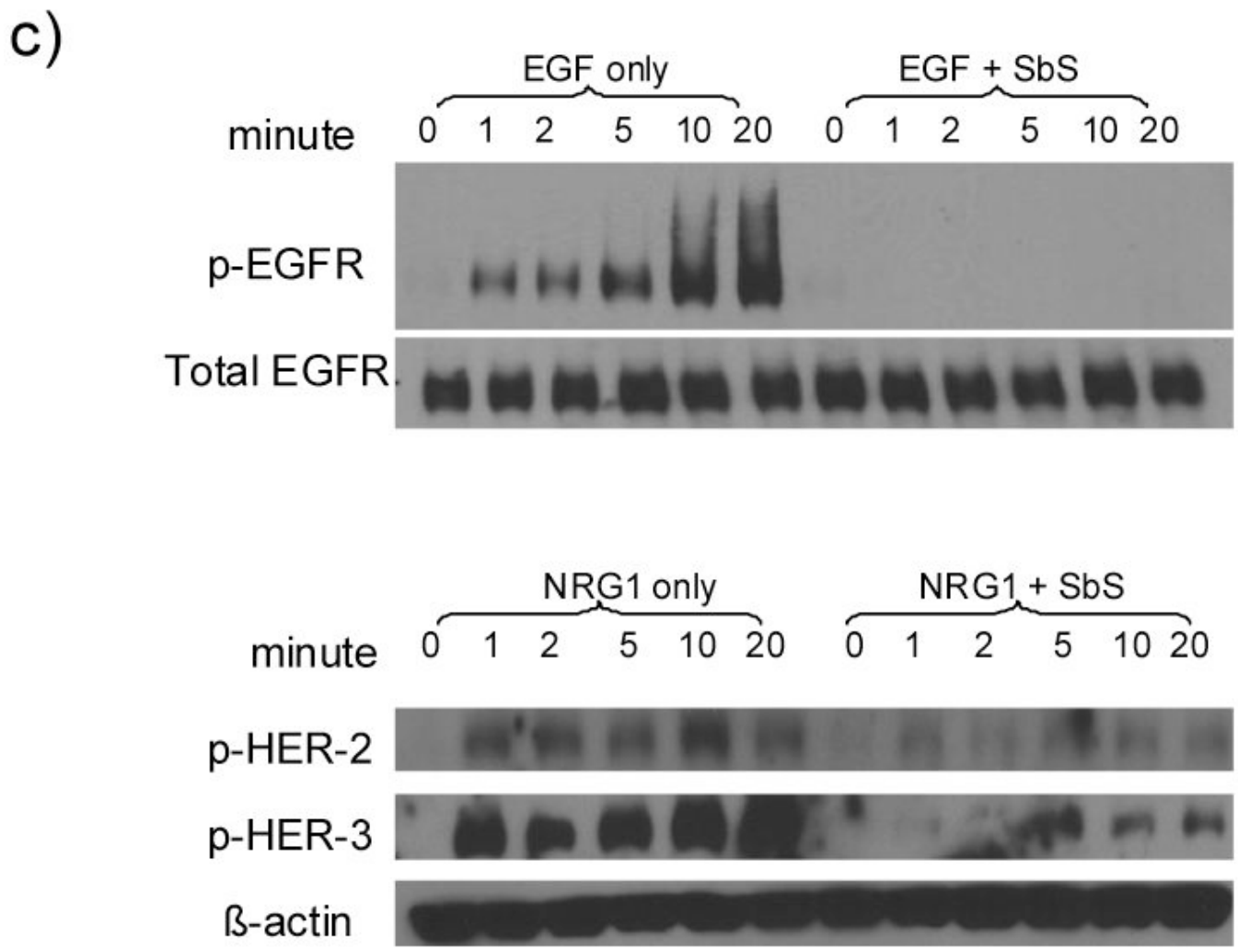

Figure 1. SbS inactivates EGFR MEK ERK signaling in colon cancer cells

a) HT29 cells grown in complete media with serum were exposed to SbS for varying periods (0 to 180 minutes) and were then harvested. Cell extracts were prepared and Western blotting was performed using either phospho- specific or total EGFR, MEK1/2, ERK1/2, or CamKII antibodies. Unless otherwise noted, antibodies against p-EGFR(Tyr1173) used.

b) HT29, SW480 or HCT-116 cells were exposed to SbS at various time points (0, 1, 2, 5, 10 and 20 minutes), p-IGF-1R p-HER-2&3, and p-EGFR(Tyr1068) were blotted with specific antibodies. Series of SbS dilutions (1, 1/2, 1/4, 1/8, 1/16) were incubated with HT29 cells for 5 minutes, p-EGFR(Tyr1173) were blotted.

c) SW480 or HCT-116 cells starved overnight in serum-free media were treated by 10ng/ml recombinant EGF or 100ng/ml NRG1 ligand with or without the presence of SbS at various time points (0, 1, 2, 5, 10 and 20 minutes). p-EGFR (Tyr1173) and p-HER-2 and p-HER-3 were blotted using specific antibodies.

All results are representative of at least three independent experiments.

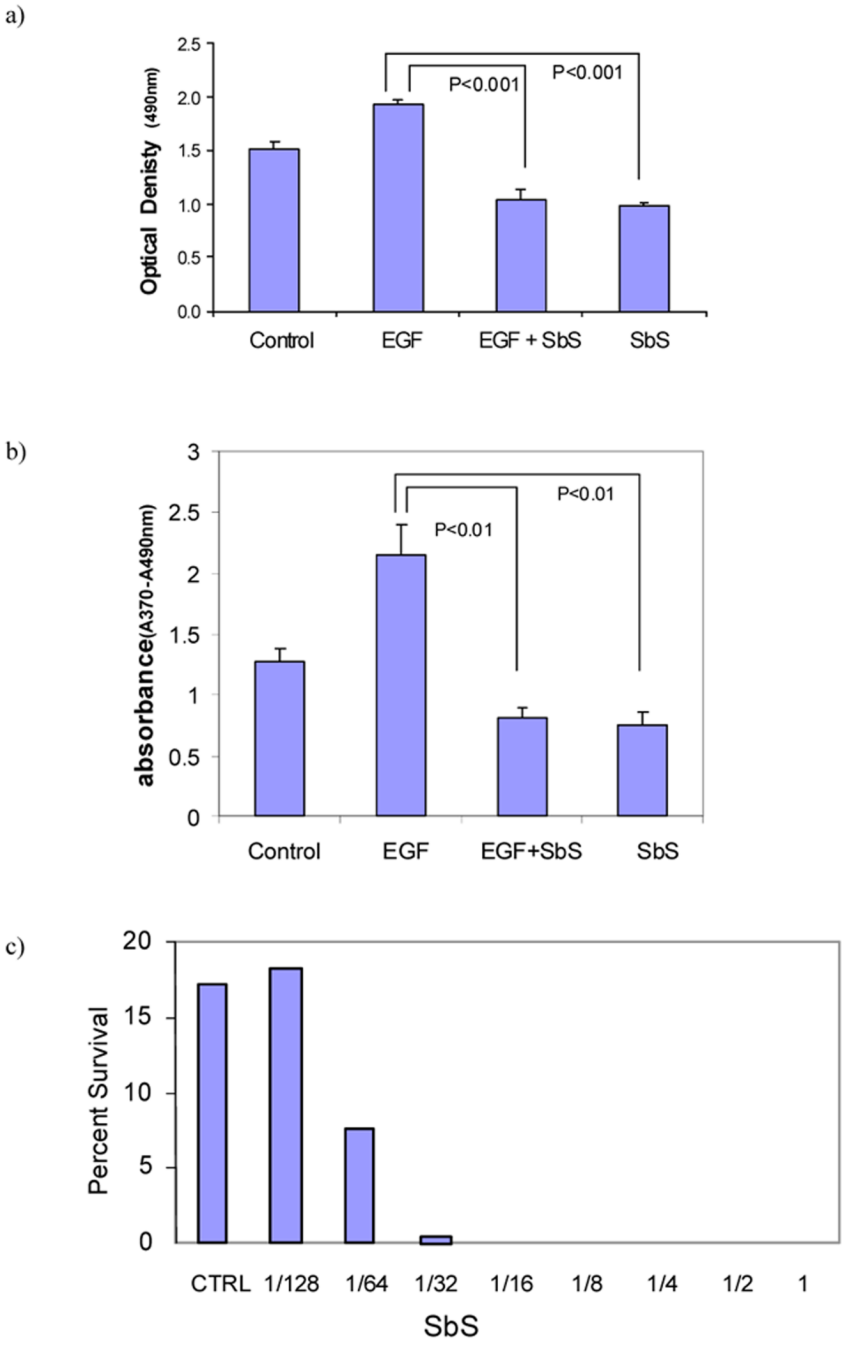

Figure 2. SbS inhibits EGF-induced cell proliferation (a&b) and prevents HT29 cell colony formation (c)

a&b) semi-confluent HT29 cells are stimulated with 10ng/ml EGF in the presence or absence of SbS for 24 hours, followed by MTS assay and colorimetric BrdU assay. Bars represent mean ± S.E.

c) Cell survival was determined by colony formation assay. HT29 cells were grown in DMEM containing 10% serum in the absence or presence of different concentrations of SbS for 10-20 days. Colonies of 30 cells or more were scored as survivors. Results are from one of two independent experiments.

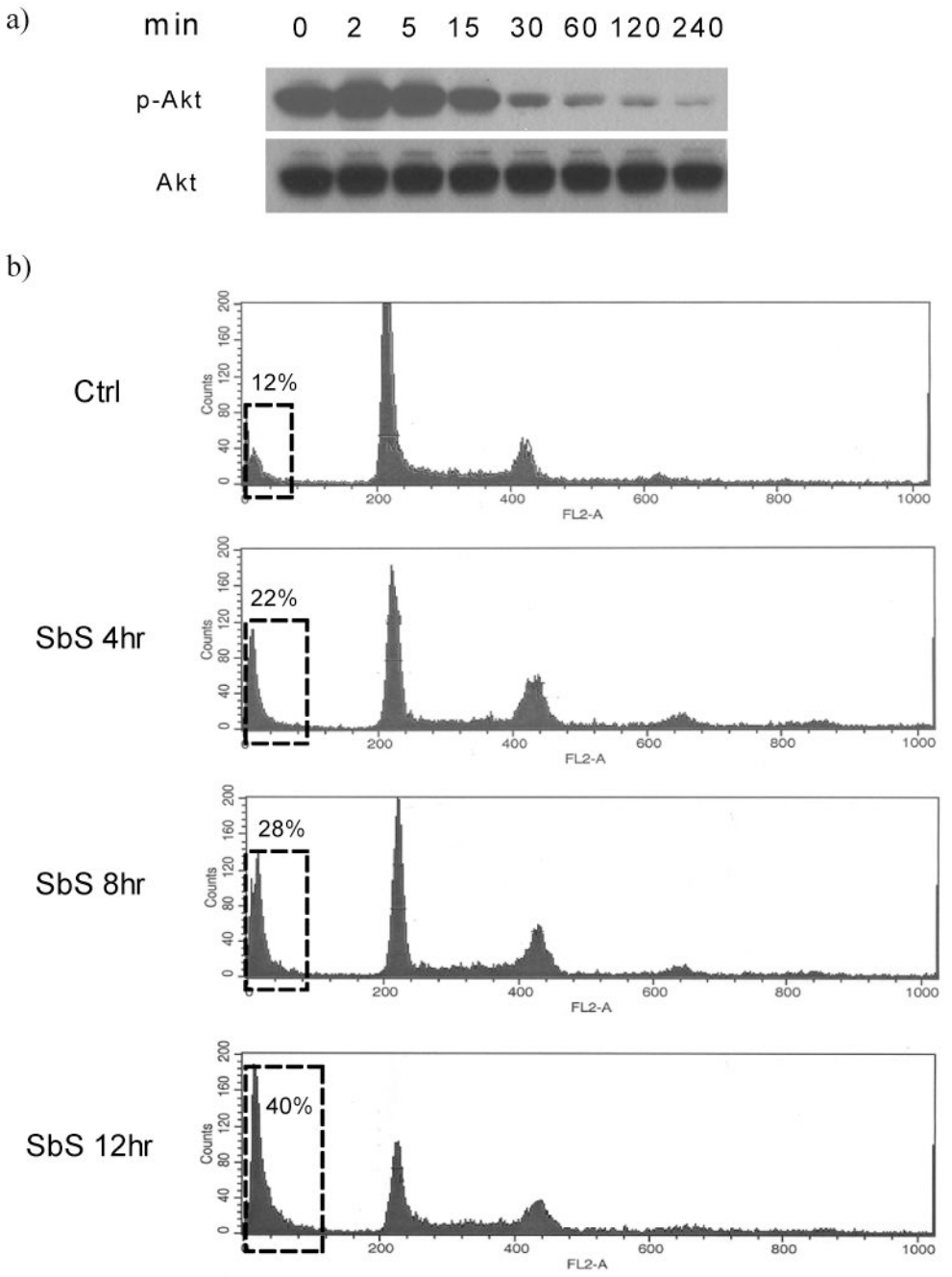

c)

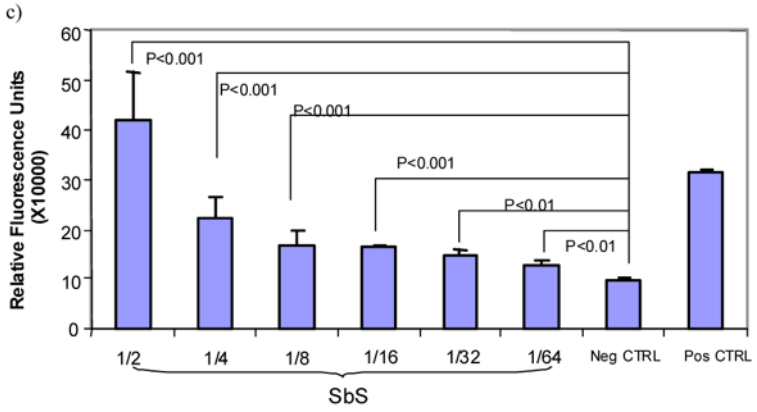

d)

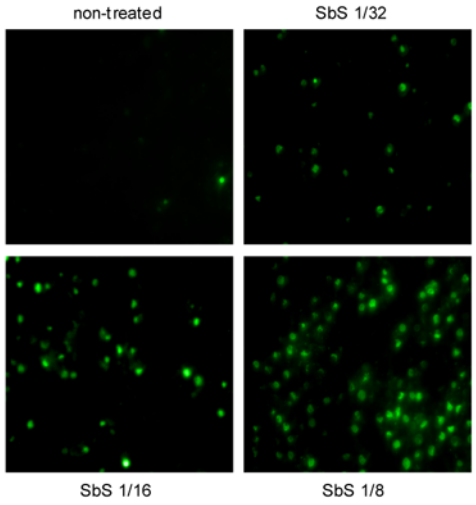

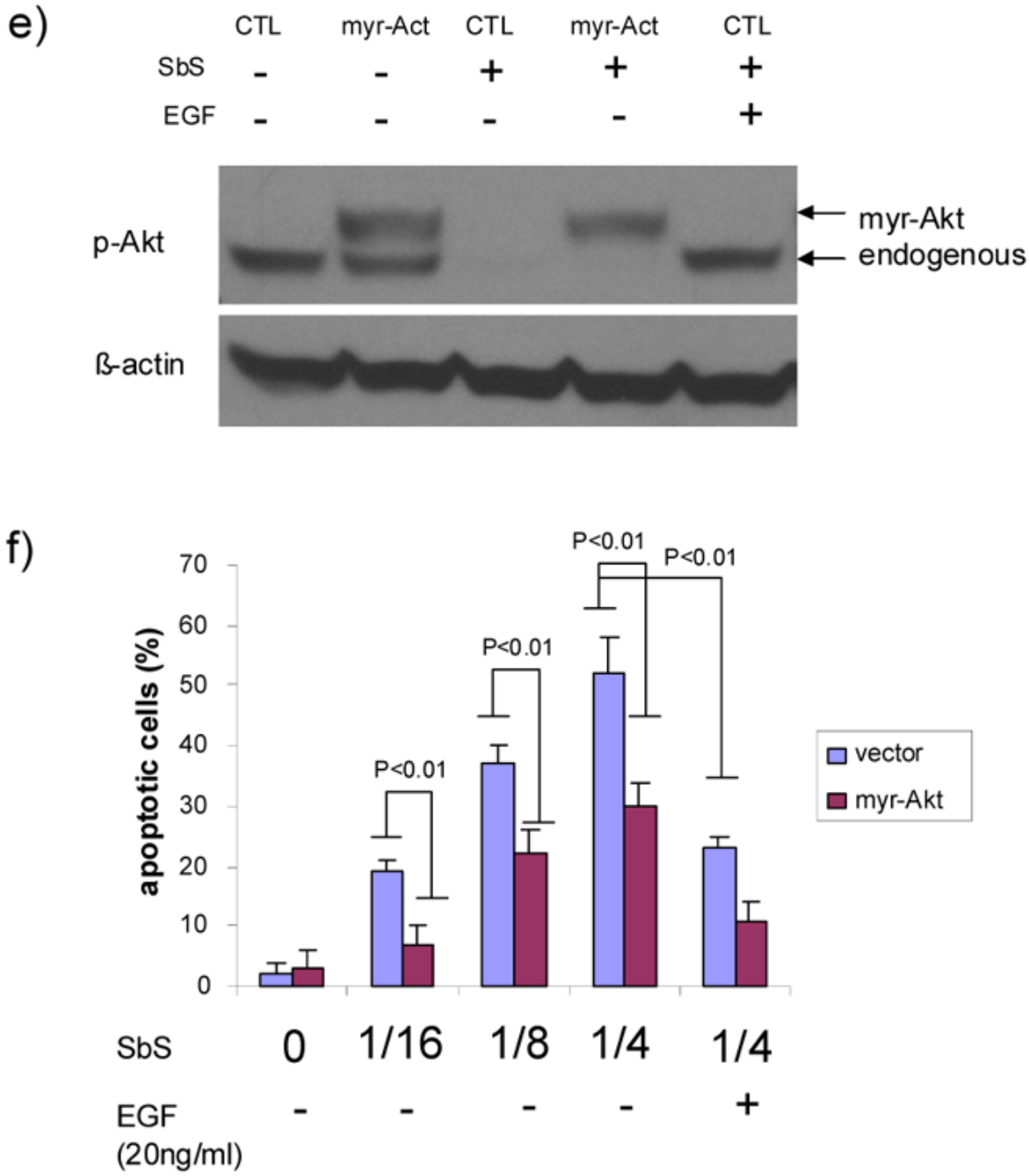

Figure 3. SbS inactivates phopho-Akt and induces HT29 cell apoptosis

a) After varying periods of time (0 - 240 min) of exposure to SbS, HT29 cells were lysed and samples tested by Western blotting using antibodies against total and phopho-Akt.

b) Human colonic cancer cells were treated with SbS for different time periods (4, 8, 12 hours), harvested and stained by propidium iodide followed by flow cytometric analysis. Cells treated with RPMI for 12 hours were used as a control. Apoptosis was determined by the sub-G_1 fraction (in rectangular boxes in figure). Results are from one of two independent experiments.

c) HT29 cells treated with SbS for 4 hours at varying dilutions (1/2 to 1/64) were then tested using homogenous caspase assay kit (Roche Applied Science). Cells treated with vehicle serves as negative control. Cells treated with 4 μg/ml camptothecin serve as positive control. Bars

represent mean ± S.E. $p < 0.01$ between SbS treated groups (at all tested doses) *versus* negative control.

d) HT29 cells treated with SbS for 12 hours at varying dilutions (1/8, 1/16, 1/32) were tested for apoptosis by tunel assay using TUNEL apoptosis detection kit. Cells labeled with green fluorescence are those undergoing apoptosis. The average percentage of positively stained cells in those treated with SbS (1/8 dilution) is 32.0±8.5%, vs. control cells 1.5±0.5%, ($p<0.01$). Representative images are shown in 3d.

e) 24 hours after HT29 cells were transfected with pUSE empty vector or pUSE-Akt, cells were treated with SbS at 1/2 dilution for 30mins then lysed for Western blotting using p-Akt. SbS decreased endogenous p-Akt signal whereas ectopic myr-Akt remained intact. Co-treatment of cells with EGF (20ng/ml) reversed the p-Akt signal reduction induced by SbS

f) HT 29 cells transiently transfected with vector or myr-Akt were treated with different dilutions of SbS for 12 hours. Apoptotic cells were then analyzed by Tunel staining. The percentage of Tunel positive cells were averaged in three independent experiments. Both ectopic myr-Akt expression and stimulation by 20ng/ml EGF ligand reduced SbS-induced apoptosis. Bars represent mean ± S.E.

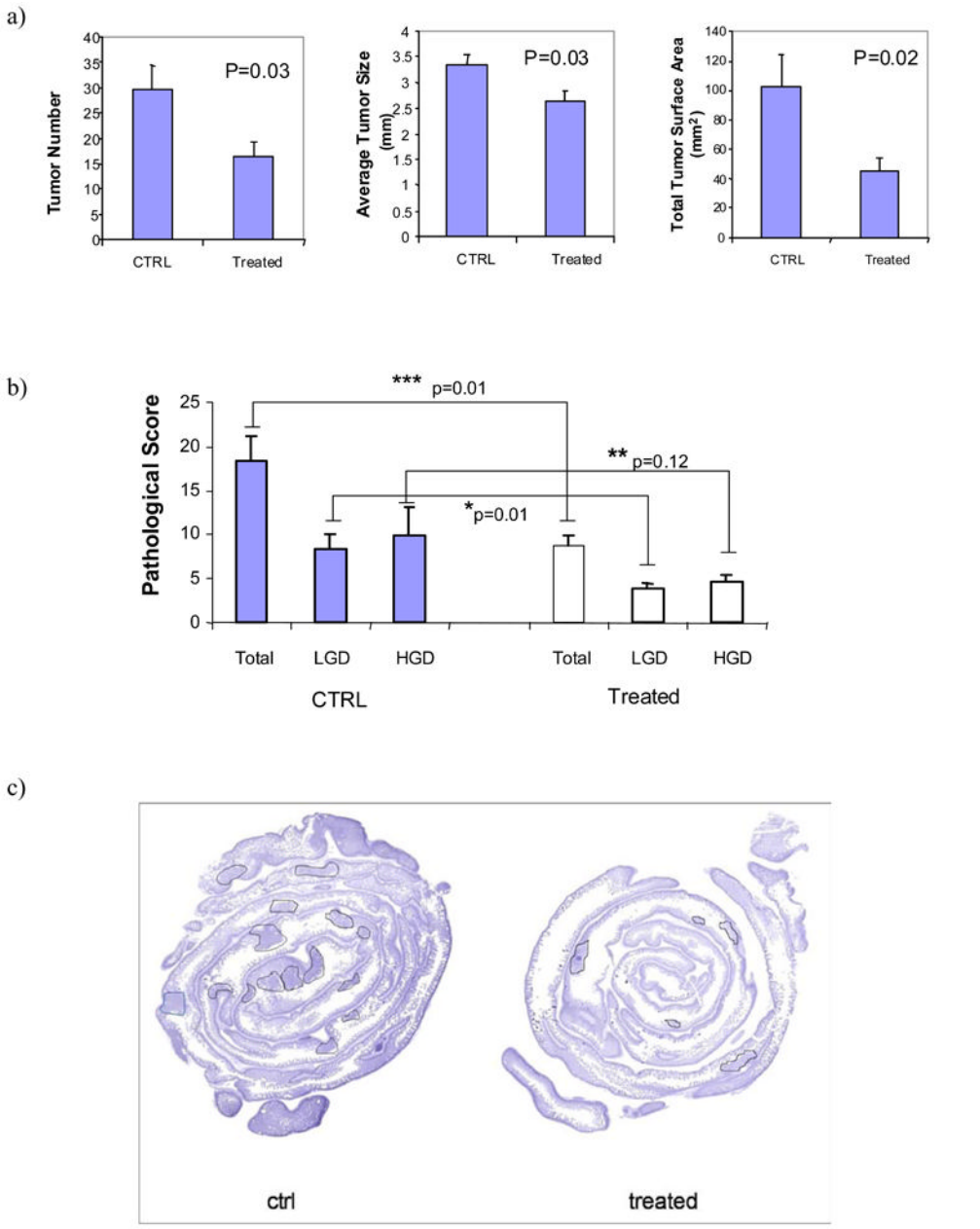

Figure 4. Oral intake of Sb inhibited tumor growth in *Apc*^{Min} mice

a) After 9 weeks of oral administration of *Sb*, *Apc*^{Min} mice were sacrificed and the 10 cm section of the distal small intestine was harvested, from which we measured the number and size of intestinal tumors. Tumor number is significantly reduced in *Apc*^{Min} mice treated with *Sb* (N=8) compared to control untreated *Apc*^{Min} mice (N=6, p=0.03). Tumor size is also significantly reduced in the treated group (p=0.03), as well as total tumor surface area (p=0.02). Bars represent mean ± S.E.

b) Using a system based on human colonic carcinoma profiles, we categorized the intestinal tumors into low grade dysplasia (LGD), high grade dysplasia (HGD) and total pathological score (LGD + HGD). *Sb*-treated *Apc*^{Min} mice had a significantly lower LGD compared to control mice (p=0.01). Scores for high grade dysplasia were also lower than in the control

group but this difference did not reach statistical significance (p=0.12). Total dysplasia score is significantly lower in the *Sb*-treated mice (p=0.01).

c) The proximal sections of the small intestines were H&E stained. Representative images illustrates the contrast between *Sb*-treated Apc^{Min} mice and control Apc^{Min} mice. Visible tumors were outlined by circles.

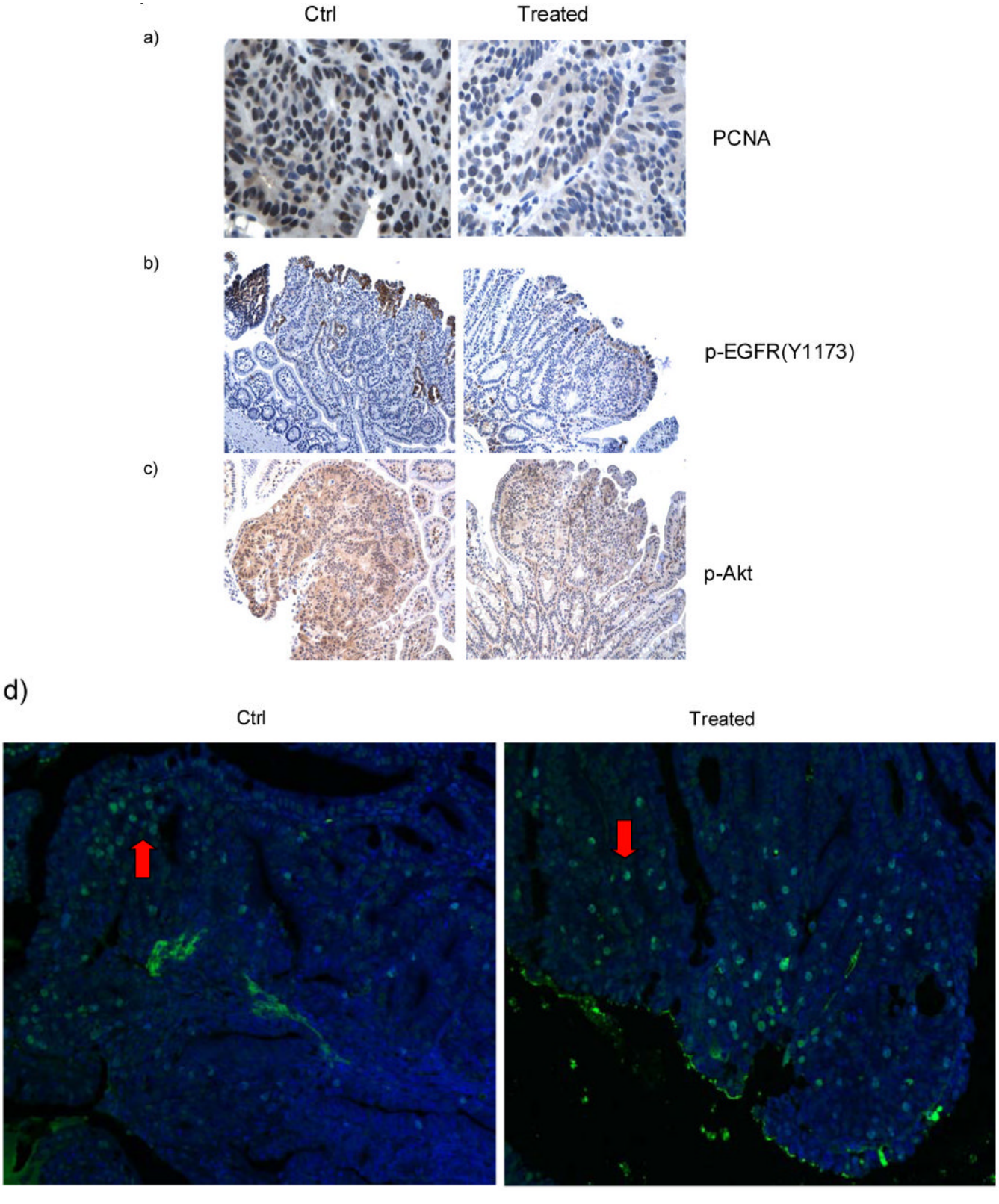

Figure 5. Immunohistochemical staining showing the *in vivo* effect of *Sb* on EGFR and Akt phosphorylation and on cell proliferation in the intestinal tumors of Apc^{Min} mice

a) The murine small intestines were stained using PCNA antibodies and counter-stained with haematoxylin. Dark/black colored nuclear staining indicates PCNA positive cells. Cells with blue colored nuclei are PCNA negative. Semi-quantative analysis using 5 representative images from each group showed that tumors from *Apc*^{Min} mice treated with *Sb* possess fewer proliferative cells compared to those from control mice (37 ± 20 % vs. 66 ± 14%, $p<0.01$).
b&c) Antibodies against Phospho-EGFR(Y1173) and Phospho-Akt were used to stain the intestinal tumors counter-stained with haemotoxylin. From microscopic views of 10 tumors from each group, the percentage of phospho-EGFR (Tyr1173) positive cells per high power field in *Sb*-treated mice vs. control mice are 6.5 ± 2.8 % vs. 17 ± 5.5 %, (mean ± S.E., $p<0.05$). The average percentage of p-Akt strongly stained cells per high power field from *Sb*-treated mice vs. control mice are 49.6 ± 5.4% vs. 70.4 ± 4.5%, $p=0.01$. Representative images are shown to compare the different staining intensity for p-EGFR and p-Akt between treated and control *Apc*^{Min} mice. (Brown color = Phospho-EGFR or Phospho-Akt).
d) Tunel staining of intestinal tissues from *Sb*-treated and control Apc^{min} mice. FITC (green) labeled cells are apoptotic tumor cells with DAPI (blue) staining as background. From 10 microscopic views each from the treated and control groups, the average percentages of apoptotic cells per high power field are 15 ± 3.0% in *Sb*-treated mice, vs. 4.5 ± 2.3 % in control mice respectively, (mean ± S.E., $p<0.01$). Representative tunnel staining images are shown Figure 5d with red arrow pointing to apoptotic cells within the tumors.